Modeling positive ion current to a planar probe in low-pressure electronegative discharges

T. H. Chung[a)]
Department of Physics, Dong-A University, Busan 604-714, Korea

(Received 17 February 2009; accepted 14 May 2009; published online 4 June 2009)

A fluid model is utilized to describe the plasma-sheath boundary for a negatively biased planar probe immersed in electronegative plasmas. The model equations are solved on the scale of the electron Debye length and calculate the spatial distributions of electric potential, velocity, and density of positive ions in front of the probe. The position of sheath edge, the positive ion velocity at sheath edge (the Bohm velocity), and the positive ion flux collected by the probe are determined and compared with analytic (or scaling) formulas. Effects of control parameters on the Bohm velocity, the sheath thickness, and on the positive ion flux are investigated. A larger thermal motion of negative ions causes the Bohm velocity to increase, the sheath to increase, and the positive ion flux collected by the probe to increase. An increase in collision causes the Bohm velocity to decrease and the sheath to decrease resulting in a decrease in the positive ion flux. An increase in electronegativity causes both the Bohm velocity and the sheath thickness to decrease, resulting in an increase in the positive ion flux. As the value of the non-neutrality parameter q increases, the Bohm velocity and the sheath thickness are found to decrease, and the positive ion flux collected by the probe increases. The behavior of the positive ion flux entering the sheath is discussed as functions of control parameters. A careful comparison of theoretical positive ion flux with the experimental flux can allow us to obtain the electronegativity, the plasma ionization rate (q), and the collision parameter (δ). © *2009 American Institute of Physics*. [DOI: 10.1063/1.3148832]

I. INTRODUCTION

Electronegative plasmas have been used extensively for many applications of plasma processing. Some important issues in electronegative plasmas include the problem of determining the electronegativity of plasmas, the sheath structure, and the spatial distribution of plasma species.[1–3] The flux of positive ions entering the sheath is another important quantity for plasma processing and electrostatic probe diagnostics. Probe technique is a simple and useful tool to diagnose the electronegative plasmas.

Most of the important plasma parameters such as the densities of charged species, electron temperature, plasma potential, and electron energy distribution function are obtained from electrostatic probe method. The ion saturation zone of the *I-V* characteristics of the probe is increasingly used in plasma diagnosis. The current drained by the probe in this zone is very small and reduces the perturbation that the measurement causes in the plasma. For a electronegative plasma, a careful interpretation of the *I-V* data of the probe is required.[4,5] A comparison of experimental *I-V* curve of the probe with a theoretical *I-V* curve can give a useful method of determining the plasma parameters. In order to construct a theoretical *I-V* curve of the planar probe, the plasma solution near the biased probe should be obtained.[6,7]

The problem of the plasma-sheath transition is still the subject of numerous recent investigations.[8] This is partly due to singularity caused by the representations of various effects (collision, space charge, and ion temperature). The variation in plasma variables in the plasma-wall transition region can be characterized with several scale lengths.[9] The ionization length or the ion mean free path can be used for observing the variation in plasma variables in the presheath region. On the other hand, the electron Debye length can be used as a scale length for the sheath region since the sheath width extends only a few electron Debye lengths.[10]

The theoretical model of the sheath structure for probes immersed in low-pressure electronegative plasmas has been developed by several authors in cylindrical or spherical geometry[6,7,11–16] and in plane geometry.[17–24] The use of the plasma approximation in the presheath region has produced rich theoretical observations of the oscillatory electric potential and stratified presheath.[12–14,18,19,21–23] Some authors insisted that these oscillations can be attenuated with the consideration of collision and finite thermal motion of positive ions.[18]

In previous papers,[10,25] fluid models for collisionless plasmas with cold positive ions and weakly collisional plasmas with a finite ion temperature were developed for studying the structure of the plasma-cylindrical probe boundary in low-pressure electronegative discharges. In this study, the model is extended to include collision of positive ions with neutrals for plasma-plane probe boundary. The spatial distributions of electric potential, velocity, and density of positive ions are calculated in front of a negatively biased planar probe immersed in electronegative plasmas. The control parameters are the ratio of the negative ion density to the electron density, the ratio of the electron temperature to the negative ion temperature, and the ratio of the momentum transfer collision frequency to the ionization frequency.

[a)]Electronic mail: thchung@dau.ac.kr.

From the calculated results, the position of sheath edge, the positive ion velocity at sheath edge, and the positive ion current collected by the probe are determined and compared with analytic (or scaling) formulas. Especially, the effects of these control parameters on the positive ion current collected by the probe are investigated. The effect of the non-neutrality parameter defined as the ratio between the electron Debye length and the ionization length is also discussed. Summarizing the effects of the control parameters, a scaling behavior of the positive ion flux emanating from electronegative discharges will be discussed as functions of control parameters. Finally, a possible application of this formulation to the probe experiments is suggested.

II. MODEL EQUATIONS

The plasma variables are calculated along the distance from the plasma region to any arbitrary small distance near the planar probe using a set of coupled equations including the steady state fluid equations of continuity and motion for the positive ion, Poisson equation with Boltzmann electron and Boltzmann negative ion.[18,19]

A fluid model for the spatial distributions of the electric potential and the density and velocity of positive ions in front of a planar probe immersed in electronegative plasmas is developed without the quasineutral approximation. For simplicity, we consider that electronegative plasma consists of three charged species, which are positive ion, negative ion, and electron.

The model equations are developed for a planar probe with the assumption of one-dimensional motion of positive ions toward the probe. The cold positive ion is assumed. The neutral gas density and the temperatures of the electrons and negative ions are taken as constant. The basic equations for the positive ions are the continuity

$$\frac{d}{dx}(n_+v_+) = \nu_{iz}n_e \tag{1}$$

and the equation of momentum transfer

$$m_+n_+v_+\frac{dv_+}{dx} = -en_+\frac{d\phi}{dx} - m_+n_e\nu_{iz}v_+ - m_+n_+\nu_c v_+, \tag{2}$$

where x denotes the position in the direction normal to the probe plane, n_+, m_+, and v_+ are the density, the mass, and the velocity of the positive ion, n_e is the electron density, ν_{iz} and ν_c are the ionization frequency and the momentum-transfer collision frequency, and ϕ is the electric potential. The second term on the right-hand side of Eq. (2) represents the decrease in fluid momentum as positive ions are born at rest.[20] The third term represents a drag force due to collisions between positive ions and neutrals.

The Poisson's equation is written as

$$\varepsilon_0\frac{d^2\phi}{dx^2} = -e(n_+ - n_e - n_-), \tag{3}$$

where ε_0 is the permittivity of the vacuum, n_- is the negative ion density, and e is the electron charge.

We assume that electrons and negative ions follow the Boltzmann energy distribution,

$$n_e = n_{e0}\exp\left(\frac{e\phi}{kT_e}\right), \tag{4}$$

$$n_- = n_{-0}\exp\left(\frac{e\phi}{kT_-}\right), \tag{5}$$

where T_e and T_- are the temperature of the electrons and the negative ions and k is the Boltzmann constant. The subscript 0 indicates the value at the plasma region.

In order for the Boltzmann relation for negative ions to hold, the condition

$$\Gamma_- \ll D_-\frac{dn_-}{dx} \tag{6}$$

must hold. Neglecting the recombination the negative ion flux is written as

$$\Gamma_- = \int K_{\text{att}}n_en_g dx, \tag{7}$$

where D_- and K_{att} are the diffusion coefficient of negative ions and attachment coefficient, respectively. The validity of this condition will be discussed in Sec. III.

The solution of the model equations describes the structure of the presheath and sheath regions in front of a planar probe. We have the dimensionless functions and parameters

$$\xi = \frac{x}{\lambda_D},\quad \tilde{n} = \frac{n_+}{n_{e0}},\quad u = \frac{v_+}{c_s},\quad \eta = -\frac{e\phi}{kT_e},\quad \alpha_0 = \frac{n_{-0}}{n_{e0}},$$
$$\gamma_- = \frac{T_e}{T_-},\quad q = \frac{\lambda_D}{\Lambda},\quad \delta = \frac{\nu_c}{\nu_{iz}}, \tag{8}$$

where c_s is the ion acoustic speed $(=\sqrt{kT_e/m_+})$, λ_D is the Debye length, and $\Lambda = c_s/\nu_{iz}$ is the ionization length. The q, sometimes called the non-neutrality parameter, is a measure of the ionization rate.

The dimensionless equations of ion continuity and momentum balance for positive ion and Poisson's equation are written as

$$\frac{d}{d\xi}(\tilde{n}u) = qe^{-\eta}, \tag{9}$$

$$u\frac{du}{d\xi} = \frac{d\eta}{d\xi} - \frac{que^{-\eta}}{\tilde{n}} - q\delta u, \tag{10}$$

$$\frac{d^2\eta}{d\xi^2} = \tilde{n} - e^{-\eta} - \alpha_0 e^{-\gamma_-\eta}. \tag{11}$$

In the quasineutral region, the differential term of the Poisson equation (11) may be neglected. Then, we have

$$\tilde{n} - e^{-\eta} - \alpha_0 e^{-\gamma_-\eta} = 0. \tag{12}$$

This equation combined with Eqs. (9) and (10) is used to obtain the initial condition,

$$[(e^{-\eta} + \alpha_0 e^{-\gamma_-\eta}) - u^2(e^{-\eta} + \alpha_0\gamma_- e^{-\gamma_-\eta})]\frac{d\eta}{d\xi}$$
$$= 2que^{-\eta} + q\delta u(e^{-\eta} + \alpha_0 e^{-\gamma_-\eta}), \tag{13}$$

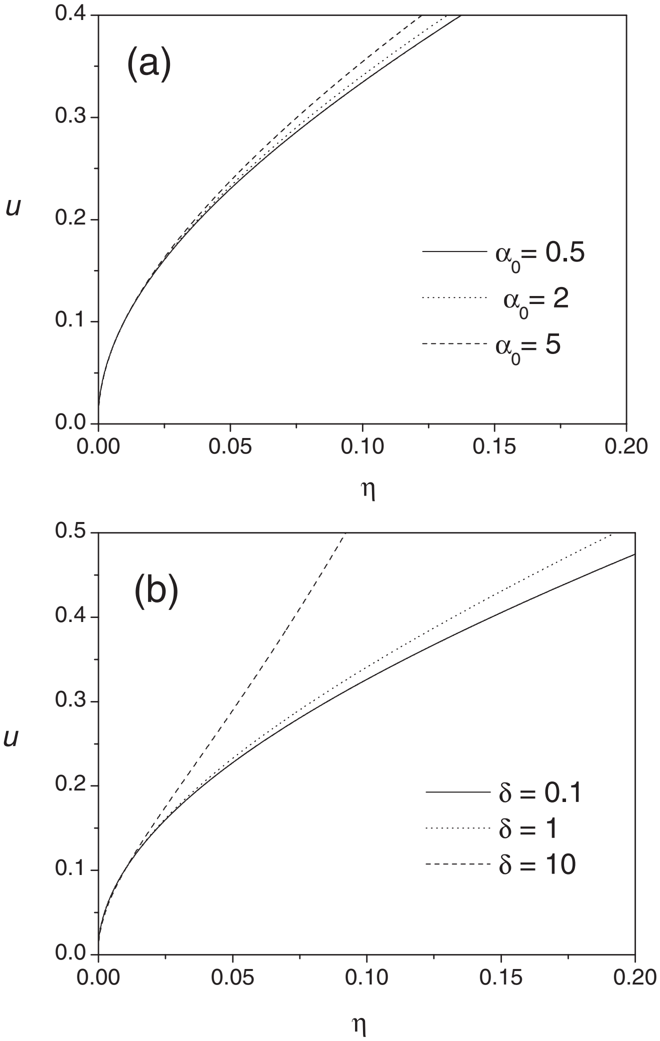

FIG. 1. The evolution of u with η near the plasma sheath transition region for (a) several α_0 and (b) several δ, where $\gamma_-=10$, $\delta=1$, and $q=0.01$ for (a) and $\alpha_0=2$ for (b).

$$[2ue^{-\eta}+\delta u(e^{-\eta}+\alpha_0 e^{-\gamma_-\eta})]\frac{du}{d\eta} = e^{-\eta}+u^2(e^{-\eta}+\alpha_0\gamma_- e^{-\gamma_-\eta})\left(\delta+\frac{e^{-\eta}}{e^{-\eta}+\alpha_0 e^{-\gamma_-\eta}}\right). \tag{14}$$

Integrating Eq. (14) with the initial value $u=0$ at $\eta=0$, we obtain u as a function of η. It should be noted that the initial condition to the model equations (9)–(11) depends on α_0, δ, γ_-, and q. Figure 1(a) shows the calculated evolution of u with η for several α_0 with $q=0.01$, $\gamma_-=10$, and $\delta=1$. Generally, with smaller α_0, the slope of the curves becomes smaller. As shown in Fig. 1(b), with smaller δ, the slope of the curves becomes smaller. The evolution of u with η has sensitive dependence on α_0 and δ. However, the value of γ_- has an insignificant influence on the evolution of u with η, and the q value has no effect on that. These plots provide the initial conditions to the model equations (9)–(11). The initial condition is chosen for values of u and η small enough corresponding to a point close to the undisturbed plasma. At this point, the value of ξ is a little displaced from 0 since we assume that $u=0$ at $\eta=0$, and thus $\xi=0$ at that point. In this work, typical initial values of u, η, and $d\eta/d\xi$ are 0.050 234, 0.0023, and 0.000 857, respectively. These values vary a little depending on the parameters (γ_-, δ, and α_0). Since the initial value of η is very small, the assumption that the initial values of $\xi=0$ and $\tilde{n}=1+\alpha_0$ can be used to solve Eqs. (9)–(11).

III. RESULTS AND DISCUSSION

The main focus of this paper is placed on the investigation of the effects of collision in the presheath, ionization rate, and electronegativity on the spatial distributions of the electric potential and the velocity and the density of positive ions toward the planar probe. For that purpose, the equations (9)–(11) are solved numerically by using the fourth-order Runge–Kutta method with the initial condition which is obtained by solving the quasineutral equations (13) and (14).

As an example of the electronegative plasma, we can consider an oxygen discharge with $p=10$ mTorr, $T_e=4$ eV; we have $c_s=3\times10^5$ cm/s, $\nu_{iz}=10^6$ s^{-1}, and $\Lambda=0.3$ cm. If $n_e=2.4\times10^{11}$ cm^{-3}, we have $\lambda_D=0.003$ cm, and $q=0.01$.

On the presheath scale the equation (6) can be written as

$$\Lambda^2 \ll \frac{D_- n_-}{K_{\mathrm{att}} n_g n_e}. \tag{15}$$

For the oxygen discharge above with $K_{\mathrm{att}}=10^{-10}$ cm^3/s, $D_-=3000$ cm^2/s, and a moderate value of α_0, this condition is easily fulfilled and the Boltzmann relation for negative ions is valid. The spatial distributions of the normalized potential, the normalized density, and the normalized velocity and flux of positive ions entering the probe are calculated for various values of γ_-, δ, α_0, and q.

Since the sheath edge is defined by a field singularity $d\eta/d\xi\to\infty$ in the quasineutral region, from Eq. (13), the Bohm criterion for the electronegative plasmas with cold positive ions becomes

$$u_s^2 \geq \frac{1+\alpha_s}{1+\alpha_s\gamma_-}, \tag{16}$$

where subscript s means the value at the sheath edge. Here, the sheath edge can also be defined as either the point at which the curvature of the electric potential becomes maximum or the point at which the positive ions reach the speed of sound in the medium (the supersonic ion criterion).[7] The sheath width (d) scales as[26]

$$\frac{d}{\lambda_D} \propto \left(\frac{Y}{3}+1\right)\sqrt{Y}, \tag{17}$$

where $Y=\sqrt{1+\psi}-1$ and $\psi=-2e\bar{\phi}/m_+ v_{+s}^2$ ($\bar{\phi}$ is the difference between the plasma potential and the probe potential). Since this equation was derived for collisionless electropositive plasmas, it has a limited use.

For collisional electropositive plasmas, the Bohm velocity becomes[27]

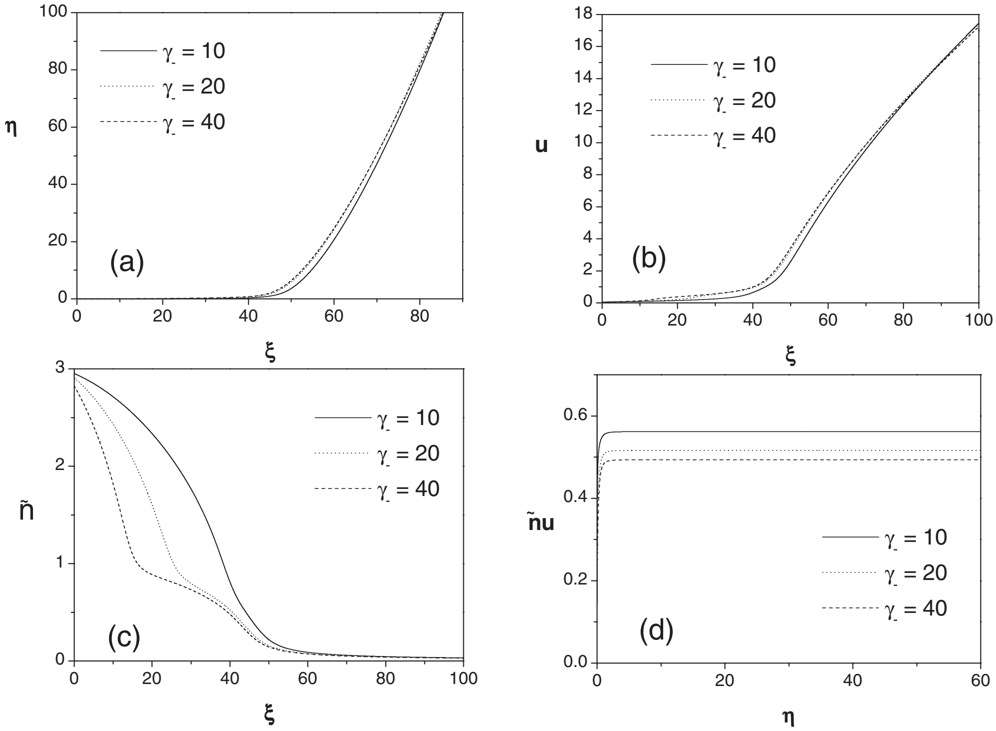

FIG. 2. (a) Normalized potential, (b) normalized velocity, (c) normalized density along the normalized distance, and (d) normalized positive ion flux vs normalized potential for various negative ion temperatures (γ_-=10, 20, and 40). Here q=0.01, α_0=2, and δ=1.

$$u_s = \frac{1}{\sqrt{1+\frac{\pi}{2}q\delta}}, \tag{18}$$

and the sheath width scales as

$$d \propto \lambda_i^{1/5}\frac{\bar{\phi}^{3/5}}{(n_{+s}v_{+s})^{2/5}}, \tag{19}$$

where λ_i is the ion mean free path ($=c_s/\nu_c$).

Figures 2(a) and 2(b) show the normalized potential and the normalized velocity of positive ions along the distance from the plasma (ξ=0) to the probe calculated from the coupled equations for various values of $\gamma_-(=10,20,40)$. Here, q=0.01, α_0=2, and δ=1 are used. As the value of γ_- increases (as the negative ion temperature becomes lower for a fixed electron temperature), the electric potential and the velocity of positive ion increase slightly fast (going from the plasma to the probe), and the positive ion velocity at the sheath is observed to decrease. As the negative ions have larger thermal motion, the sheath is found to increase slightly, and the positive ion flux collected by the probe increases.[28]

Figure 2(c) shows the normalized density of positive ions along the distance for various values of γ_-. It is observed that the density profile of positive ion decreases slowly toward the probe and the sheath thickness expands as γ_- decreases. Physically speaking, as the negative ion temperature is increased (for a fixed electron temperature), the negatively charged particle flux to the probe increases slightly. Therefore, the length of non-neutral region (that is, sheath thickness) increases with decreasing γ_-. A similar phenomenon can happen when the electron temperature becomes lower for a fixed negative ion temperature. The positive ion flux to the probe increases to balance the negative charged flux; however, the dependence of the positive ion flux on the negative ion temperature is weak except for a small γ_- region.

The point on the curve of the electric potential at the probe position $\xi=\xi_p$ gives the normalized potential η_p. The model provides the dimensionless positive ion flux to the voltage characteristics by plotting $\tilde{n}_{\xi_p}u_{\xi_p}$ versus the dimensionless electric potential η_p. Figure 2(d) is a theoretical *I-V* curve plotted in this way. The positive ion saturation current density is written as

$$J_+ = en_{+s}v_{+s} = en_{e0}c_s\tilde{n}_s u_s = en_{e0}c_s\tilde{n}_{\xi_p}u_{\xi_p}. \tag{20}$$

In order to determine the positive ion density, the electron density n_{e0} and electron temperature should be known. These are supposed to be determined from the electron saturation current and the slope of the experimental *I-V* curve of the probe in the exponential region. In principle, one can obtain the values of q, α_0, δ, and γ_- by comparing the experimental $\tilde{n}_s u_s$ with the theoretical values of $\tilde{n}_s u_s$. However, there are too many control parameters q, α_0, δ, and γ_- needed to plot the theoretical *I-V* curve. We will discuss this problem in a later part.

Figures 3(a) and 3(b) show the normalized potential and the normalized velocity of positive ions along the distance for various values of $\delta(=0.1,1,10)$. Here, q=0.01, α_0=2, and γ_-=10 are used. The δ indicates the ratio of the rate coefficient for momentum transfer collision to that for the ionization. This value defines the collisionality of the plasma

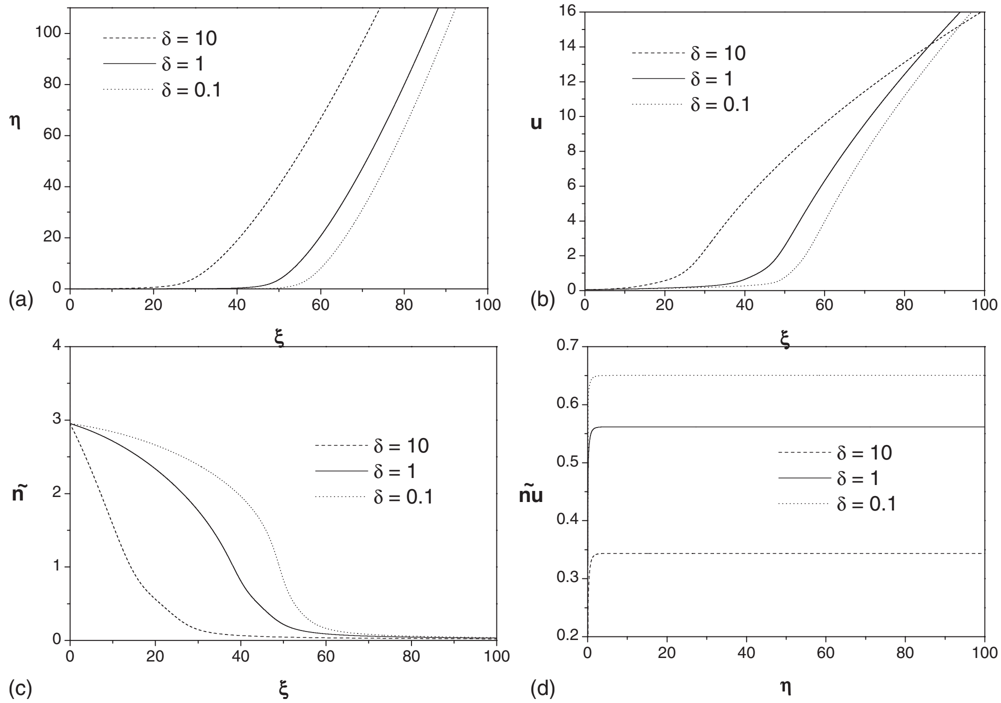

FIG. 3. (a) Normalized potential, (b) normalized velocity, (c) normalized density along the normalized distance, and (d) normalized positive ion flux vs normalized potential for various collision parameters (δ=0.1, 1, and 10). Here q=0.01, α_0=2, and γ_-=10.

and is small at low pressure, being of the order of 1 and of the order of 1000 at higher pressure.[29,30] The increase in δ (collision term) causes the electric potential and the velocity to increase more rapidly (going from the plasma to the probe). If we look at the figure carefully, we can note that both the Bohm velocity (u_s) and the sheath thickness decrease as the value of δ increases. This can be accounted for from Eqs. (18) and (19). If δ increases for a fixed $q(\nu_{iz})$, the ion mean free path (λ_i) decreases, then the sheath thickness decreases. In a physical interpretation, as the collision increases, the positive ion flux to the probe decreases resulting in a decrease in the electron flux to the probe, and thus the sheath thickness decreases with increasing δ.

Figure 3(c) shows the normalized density of positive ions along the distance for various values of δ. It is observed that the density profile of positive ion decreases drastically toward the probe and the sheath width decreases as δ increases. Figure 3(d) is a theoretical *I-V* curve for several δ. The results show that as δ increases, the positive ion flux to the probe decreases even though the sheath thickness decreases.

The normalized potential and normalized velocity of positive ions corresponding to the three different α_0(=0.5,2,5) are shown in Figs. 4(a) and 4(b). Here, q=0.01, γ_-=10, and δ=1 are used. Generally, as α_0 increases, the potential increases rapidly to higher values and the sheath thickness decreases. However, for a not largely negative probe ($\eta<30$), the case of α_0=2 has a shorter sheath thickness than that of α_0=5. This behavior was also observed in the analysis of plasma-sheath boundary for a cylindrical probe.[31] This result is in agreement with the result of Crespo *et al.*[7] and Amemiya *et al.*[11] The velocity has a similar profile to that for the normalized potential. It can be noted that the Bohm velocity decreases as the value of α_0 increases in agreement with Eq. (16). Figure 4(c) shows the density profiles of positive ions for various α_0. The density profile of positive ion is observed to decrease toward the probe more drastically for higher values of α_0. Therefore, the sheath thickness decreases with α_0 in agreement with Eq. (17). This can be accounted for by that as the negative ion density becomes larger for a fixed electron density, the length of non-neutral region close to the probe is reduced. From Fig. 4(d), it is seen that the positive ion flux collected by the probe increases with increasing α_0 since the initial value of the normalized density is $1+\alpha_0$. However, if a positive ion density (n_{+0}) is fixed with a normalization by $1+\alpha_0$, the results indicate that a lower α_0 case produces a larger positive ion flux.

Figures 5(a) and 5(b) show the profiles of the electric potential and the normalized velocity of positive ions at three different values of q(=0.005,0.01,0.1). Here, α_0=2, γ_-=10, and δ=1 are used. As q increases, more charged species are produced, thus the electric potential increases more rapidly (going from the plasma to the probe), and the sheath thickness is found to decrease. Also, as q increases the velocity of the positive ion gets larger but the Bohm velocity decreases, which is in agreement with Eq. (18). As q increases for fixed δ and λ_D, this is equivalent to a decrease in λ_i, thus both the Bohm velocity and the sheath thickness decrease.

Figure 5(c) shows the normalized density of positive ions along the distance for various parameter values of q. It is observed that the density profile of positive ion decreases rapidly toward the probe as q increases, indicating a decrease in the sheath thickness. For q=0.005 (near the plasma approximation), it is observed that the spatial profile of the positive ion density has an oscillatory structure at the early

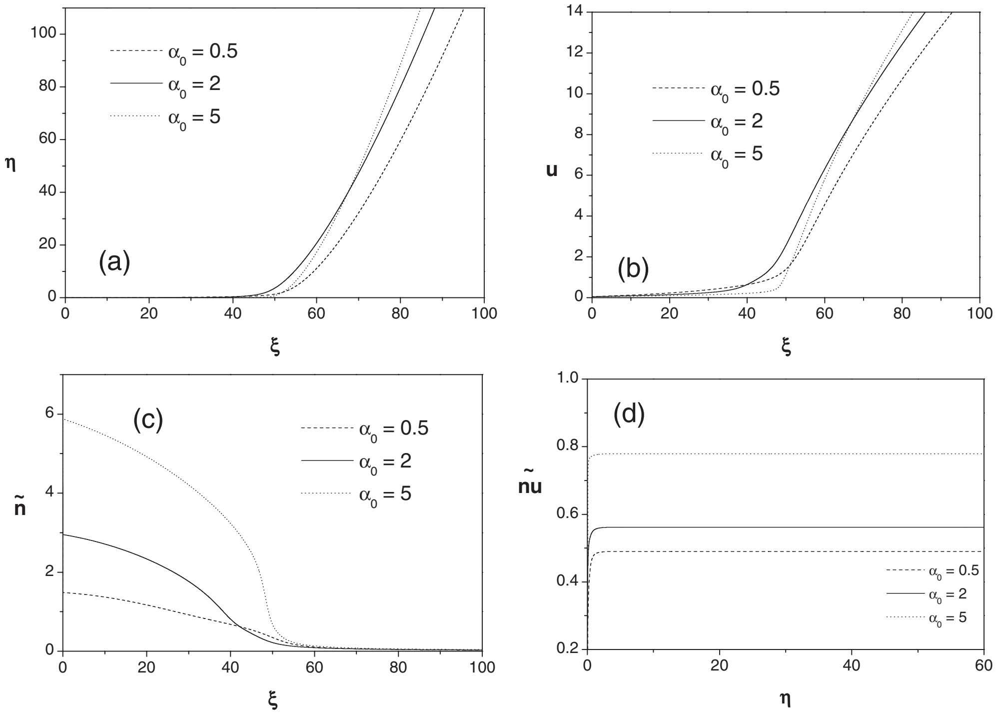

FIG. 4. (a) Normalized potential, (b) normalized velocity, (c) normalized density along the normalized distance, and (d) normalized positive ion flux vs normalized potential for various α_0 (α_0=0.5, 2, and 5). Here q=0.01, γ_-=10, and δ=1.

stage. This oscillation occurs because quasineutrality is violated while the positive ions do not satisfy the Bohm criterion.[19] However, such stationary oscillation is believed to be artifacts inherent to the fluid theory utilizing the plasma approximation.[12,18,29] From Fig. 5(d), it is seen that the positive ion flux collected by the probe increases with increasing q since larger q results in more positive ion production by ionization. The drastic increase in the positive ion velocity also contributes to an increase in the positive ion flux.

The dependence of the positive ion flux on q, α_0, δ, and γ_- is shown in Fig. 6. The solid lines represent the calculated values without the ionization source term in the momentum

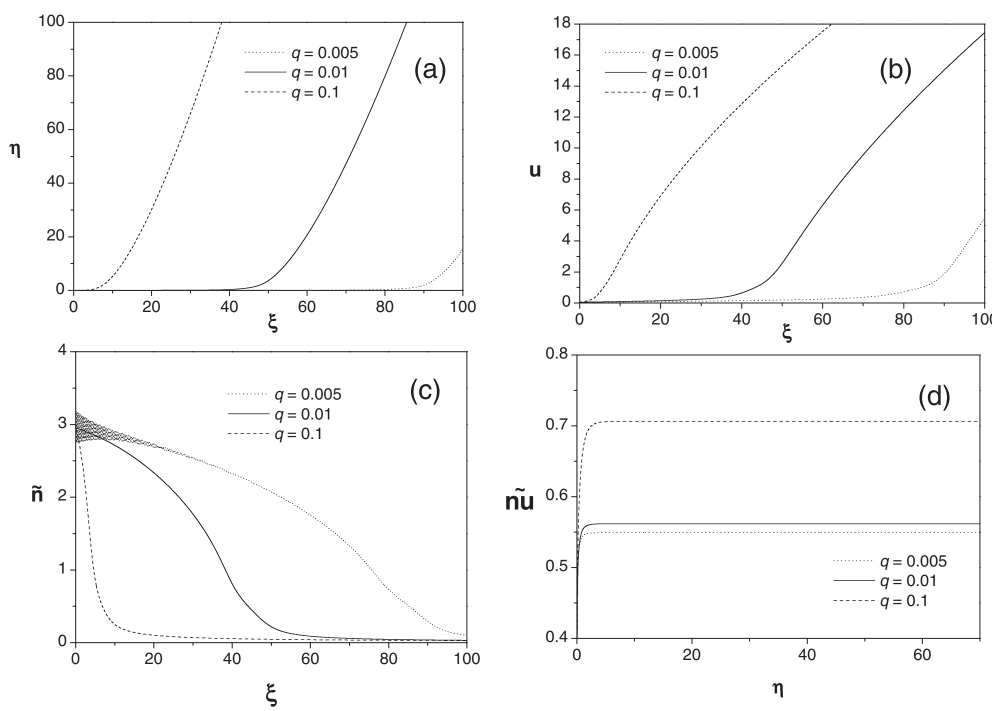

FIG. 5. (a) Normalized potential, (b) normalized velocity, (c) normalized density along the normalized distance, and (d) normalized positive ion flux vs normalized potential for various q (q=0.005, 0.01, and 0.1). Here α_0=2, γ_-=10, and δ=1.

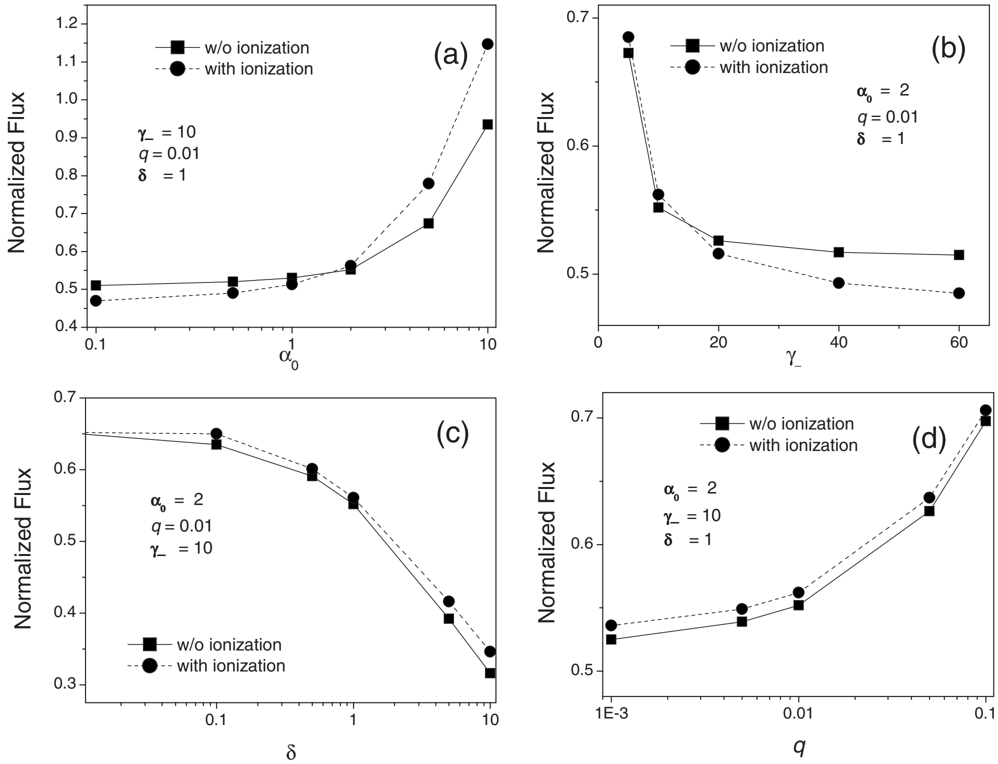

FIG. 6. Normalized positive ion flux entering the sheath as functions of (a) α_0, (b) γ_-, (c) δ, and (d) q.

balance equation, Eq. (2). The ionization source term results in a little larger value of the positive ion flux to the probe except for the $\gamma_- > 15$ and $\alpha_0 < 2$ regions. The flux increases with q and α_0 but decreases with γ_- and δ. The crucial factors influencing the flux are the Bohm velocity and the sheath thickness. The Bohm velocity increases with q but decreases with γ_-, α_0, and δ. The sheath thickness decreases with γ_-, q, α_0, and δ. The figure shows that the flux depends weakly on the control parameters each for $q < 0.01$, $\alpha_0 < 2$, $\delta < 0.5$, and $\gamma_- > 20$ regions.

The determination of electronegativity (thus, the positive ion density) can be easily proceeded by utilizing the plasma approximation. The ratio of the negative ion density to the electron density (α_0) has been determined using a novel two-probe technique.[32] The positive ion flux was measured using a guard planar probe, while the negative charge saturation current was obtained using a small cylindrical probe. The negative ion fraction was then determined from the ratio of the two currents. The negative ion fraction in the bulk plasma α_0 can be deduced from the saturation current density ratio R, which is a function of α_0 and γ_-,[33,34]

$$R = \frac{J_e}{J_+} = f(\alpha_0, \gamma_-). \tag{21}$$

Here J_e is the negative charge saturation current

$$J_e = e\left[n_{e0}\left(\frac{kT_e}{2\pi m_e}\right)^{1/2} + n_{-0}\left(\frac{kT_-}{2\pi m_-}\right)^{1/2}\right], \tag{22}$$

where m_- and m_e are the mass of negative ion and electron, respectively.

In this saturation current, the contribution of negative ions may be neglected for small and moderate α_0. This technique is simple but requires a good model for the positive ion flux to the probe. The positive ion saturation current density is again written derived as

$$J_+ = e\Gamma_s(\alpha_0, \gamma_-), \tag{23}$$

where $\Gamma_s = n_{+s} v_{+s}$ is the positive ion flux at sheath edge which depends on α_0 and γ_-.[19,32] When the plasma approximation is considered, the necessity for finding δ and q is eliminated, then we have[18,19]

$$n_{+s} = n_{e0}[e^{-\eta_s} + \alpha_0 e^{-\gamma_- \eta_s}], \quad v_{+s}^2 = c_s^2 \frac{e^{-\eta_s} + \alpha_0 e^{-\gamma_- \eta_s}}{e^{-\eta_s} + \alpha_0 \gamma_- e^{-\gamma_- \eta_s}}, \tag{24}$$

where η_s is the normalized sheath edge potential

$$\eta_s = \frac{1 + \alpha_0 e^{-(\gamma_- - 1)\eta_s}}{2(1 + \alpha_0 \gamma_- e^{-(\gamma_- - 1)\eta_s})}. \tag{25}$$

From Eq. (20), we can write

$$R \simeq \left(\frac{m_+}{2\pi m_e}\right)^{1/2} \frac{n_{e0} c_s}{\Gamma_s(\alpha_0, \gamma_-)}. \tag{26}$$

By comparing this with the theoretical value of Γ_s, one can obtain α_0 and γ_-.

Another method for finding α_0 has been suggested recently.[35] From the current-voltage (I-V) curves of probe, the saturation currents of the positive ions and electrons and the electron temperature are measured. The electronegativity

α_0 and the negative ion density are deduced by using the ratios of these parameters at three close pressure points. With a given set of α_0 and γ_-, the comparison of theoretical ion flux with the experimental flux can be done relatively easily. A further careful comparison allows us to obtain the plasma ionization rate (q) and the collision parameter (δ).

IV. CONCLUSION

The spatial distributions of electric potential and velocity and density of positive ions are calculated in front of a negatively biased planar probe immersed in electronegative plasmas. The control parameters are the ratio of the negative ion density to the electron density, the ratio of the electron temperature to the negative ion temperature, and the ratio of the rate coefficient for the momentum transfer collision to that for the ionization. The model equations are solved on the scale of the electron Debye length. The behavior of electric potential, density and velocity of positive ion, and the positive ion flux collected by the probe are investigated as functions of control parameters and compared with the analytic (or scaling) formula. If negative ions have a larger thermal motion, the positive ion velocity at the sheath edge increases, the sheath is slightly increased, and the positive ion current collected by the probe increases. The increase in collision causes the positive ion velocity at sheath edge to decrease, resulting in a decrease in the positive ion flux. An increase in electronegativity (α_0) causes the sheath thickness to decrease, resulting in an increase in the positive ion flux. As the value of the non-neutrality parameter q increases, the sheath thickness is found to decrease, and the positive ion flux collected by the probe increases. With a given set of α_0 and γ_-, a careful comparison of theoretical positive ion flux with the experimental flux allows us to obtain the plasma ionization rate (q) and the collision parameter (δ).

ACKNOWLEDGMENTS

This work was supported by the research grant of Dong-A University.

[1] T. H. Chung, H. J. Yoon, and D. C. Seo, J. Appl. Phys. **86**, 3536 (1999).
[2] T. H. Chung, D. C. Seo, G. H. Kim, and J. S. Kim, IEEE Trans. Plasma Sci. **29**, 970 (2001).
[3] D. C. Seo, T. H. Chung, H. J. Yoon, and G. H. Kim, J. Appl. Phys. **89**, 4218 (2001).
[4] E. Stamate and K. Ohe, J. Appl. Phys. **84**, 2450 (1998).
[5] E. Stamate and K. Ohe, J. Appl. Phys. **89**, 2058 (2001).
[6] R. Morales Crespo, J. I. Fernández Palop, M. A. Hernández, S. Borrego del Pino, and J. Ballesteros, J. Appl. Phys. **95**, 2982 (2004).
[7] R. Morales Crespo, J. I. Fernández Palop, M. A. Hernández, S. Borrego del Pino, and J. Ballesteros, J. Appl. Phys. **96**, 4777 (2004).
[8] K. U. Riemann, J. Seebacher, D. D. Tskhakaya, Sr., and S. Kuhn, Plasma Phys. Controlled Fusion **47**, 1949 (2005).
[9] K. U. Riemann, IEEE Trans. Plasma Sci. **23**, 709 (1995).
[10] T. H. Chung, J. Appl. Phys. **103**, 123302 (2008).
[11] H. Amemiya, B. M. Annaratone, and J. E. Allen, Plasma Sources Sci. Technol. **8**, 179 (1999).
[12] A. Kono, J. Phys. D **32**, 1357 (1999).
[13] A. Kono, J. Phys. D **34**, 1083 (2001).
[14] J. I. Fernández Palop, J. Ballesteros, M. A. Hernández, R. Morales Crespo, and S. Borrego del Pino, J. Phys. D **38**, 868 (2005).
[15] J. I. Fernández Palop, J. Ballesteros, V. Colomer, and M. A. Hernández, J. Phys. D **29**, 2832 (1996).
[16] R. Morales Crespo, J. I. Fernández Palop, M. A. Hernández, S. Borrego del Pino, J. M. Diaz-Cabrera, and J. Ballesteros, J. Appl. Phys. **99**, 053303 (2006).
[17] R. Morales Crespo, J. I. Fernández Palop, M. A. Hernández, M. V. Lucena-Polonio, and J. Ballesteros, J. Appl. Phys. **104**, 083304 (2008).
[18] R. N. Franklin, Plasma Sources Sci. Technol. **9**, 191 (2000).
[19] T. E. Sheridan, P. Chabert, and R. W. Boswell, Plasma Sources Sci. Technol. **8**, 457 (1999).
[20] T. E. Sheridan, J. Phys. D **32**, 1761 (1999).
[21] A. Kono, J. Phys. D **36**, 465 (2003).
[22] J. I. Fernández Palop, J. Ballesteros, M. A. Hernández, R. Morales Crespo, and S. Borrego del Pino, J. Phys. D **37**, 863 (2004).
[23] J. I. Fernández Palop, J. Ballesteros, M. A. Hernández, and R. Morales Crespo, Plasma Sources Sci. Technol. **16**, S76 (2007).
[24] J. I. Fernandez Palop, J. Ballesteros, R. Morales Crespo, and M. A. Hernandez, Appl. Phys. Lett. **88**, 261502 (2006).
[25] T. H. Chung, Phys. Plasmas **13**, 024501 (2006).
[26] J. L. Jauberteau and I. Jauberteau, Plasma Sources Sci. Technol. **17**, 015019 (2008).
[27] M. A. Lieberman and A. J. Lichtenberg, *Principles of Plasma Discharge and Materials Processing* (Wiley, New York, 1994), p. 171.
[28] J. I. Fernández Palop, J. Ballesteros, M. A. Hernández, R. Morales Crespo, and S. Borrego del Pino, J. Appl. Phys. **95**, 4585 (2004).
[29] R. N. Franklin and J. Snell, J. Phys. D **33**, 1990 (2000).
[30] R. N. Franklin, J. Phys. D **36**, 2821 (2003).
[31] T. H. Chung, "Modeling the plasma-sheath boundary for a cylindrical probe in electronegative plasmas," J. Korean Phys. Soc. (to be published).
[32] P. Chabert, T. E. Sheridan, R. W. Boswell, and J. Perrins, Plasma Sources Sci. Technol. **8**, 561 (1999).
[33] N. St. J. Braithwaite and J. E. Allen, J. Phys. D **21**, 1733 (1988).
[34] R. L. F. Boyd and J. B. Thompson, Proc. R. Soc. London, Ser. A **252**, 102 (1959).
[35] S. Y. Kang, T. H. Chung, and K.-S. Chung, Rev. Sci. Instrum. **80**, 013502 (2009).